Separation Science and Technology
Publication details, including instructions for authors and subscription information:
http://www.informaworld.com/smpp/title~content=t713708471

Aqueous Micellar Solvent Extraction of Phenol from Wastewater

Marcial Cordova Figueroa[a]; Martin E. Weber[a]
[a] Department of Chemical Engineering, McGill University, Montreal, Quebec, Canada

To cite this Article Figueroa, Marcial Cordova and Weber, Martin E.(2005) 'Aqueous Micellar Solvent Extraction of Phenol from Wastewater', Separation Science and Technology, 40: 8, 1653 — 1672
To link to this Article: DOI: 10.1081/SS-200059592
URL: http://dx.doi.org/10.1081/SS-200059592

Separation Science and Technology, 40: 1653–1672, 2005

ISSN 0149-6395 print/1520-5754 online
DOI: 10.1081/SS-200059592

Aqueous Micellar Solvent Extraction of Phenol from Wastewater

Marcial Cordova Figueroa and Martin E. Weber
Department of Chemical Engineering, McGill University, Montreal, Quebec, Canada

Abstract: In aqueous micellar solvent extraction (AMSE), an organic solute is extracted from an aqueous solution across an ultrafiltration membrane into a solvent consisting of an aqueous micellar surfactant solution. The solute crossing the membrane is solubilized in the surfactant micelles, which are retained by the membrane. Phenol was extracted from water into an aqueous solution of sodium dodecyl sulfate (SDS) in hollow fiber membrane contactors of 5 K and 10 K molecular weight cutoff. The objectives were to determine the effect of bulk flow across the membrane on the transfer of phenol, and to measure the extent of back contamination of the wastewater by surfactant. Cocurrent flow of solvent and wastewater with equal transmembrane pressure differences at each end of the module were used to impose uniform bulk flows. Extractions with a range of bulk flowrates across the membrane in either direction yielded smaller overall diffusive mass transfer coefficients than the value with no bulk flow, which was approximately 2 μm/s. Back contamination of the wastewater by the surfactant was reduced by lowering the CMC of the solvent.

Keywords: Solvent extraction, hollow fiber contactor, surfactant micelles, solubilization

INTRODUCTION

Phenol is a major water pollutant because of its high toxicity and high water solubility. At low concentrations phenol can be removed from wastewater by

Received 24 February 2004, Accepted 17 February 2005
Address correspondence to Martin E. Weber, Department of Chemical Engineering, McGill University, 3610 University Street, Montreal, Quebec H3A 2B2, Canada. E-mail: martin.weber@mcgill.ca

adsorption or biological degradation. At higher concentrations, treatment is problematic because of poisoning of microbes and the cost of adsorbents. In this case, other methods may be used to reduce its concentration before biological treatment or adsorption. One candidate method is extraction because its costs are often less than distillation or catalytic oxidation.

Solvent extraction is usually carried out by direct contact of the solvent and the wastewater. Because direct contact may generate a persistent emulsion, extraction across a microporous membrane is advantageous (1, 2). To compensate for the additional mass transfer resistance imposed by the membrane, hollow fiber contactors having a large membrane area per unit volume are used (3, 4). Such contactors have been employed in the extraction of phenol from wastewater (5–7). In many extractions, the two phases leave the contactor mutually saturated; for example, Yun, Prassad, and Sirkar (8) found more than 1.5 g/L MIBK solvent in their treated wastewater from which 95% of the phenol had been extracted. Back-contamination may be reduced by using solvents of low water solubility, such as decanol (5). An alternative is to use an aqueous, micellar surfactant solution as a solvent.

In aqueous micellar solvent extraction (AMSE), an aqueous surfactant solution acts as a solvent to extract a pollutant across a microporous membrane. The concentration of the surfactant in the solvent is above its critical micelle concentration (CMC). Pollutant molecules crossing the membrane are solubilized in the surfactant micelles. The micelles are retained in the solvent by selecting an ultrafiltration membrane of appropriate molecular weight cutoff (MWCO). Since surfactant monomers may diffuse across the membrane, a surfactant with a low CMC is desirable. This process, proposed by Hurter and Hatton (9), was demonstrated by Marx and Weber (10) using hollow fiber membrane contactors. The latter authors showed that a dissolved organic solute could be extracted from an aqueous phase into a surfactant solution even when the total concentration in the solvent was larger than the concentration in the wastewater. They also found some back-contamination of the treated water by the surfactant.

Since both phases in AMSE are aqueous, there may be a bulk flow across the membrane even with a very small transmembrane pressure difference. Marx and Weber (10) carried out AMSE with countercurrent flow of solvent and wastewater. In countercurrent flow, the pressures on opposite sides of the membrane cannot be matched, hence there will always be a pressure-driven bulk flow across the membrane. Marx and Weber adjusted the flowrates of the wastewater and the solvent so that the net bulk flow across the membrane was small, i.e., the flow across the membrane out of the solvent near one end of the contactor was balanced by an equal flow across the membrane in the opposite direction near the other end of the contactor.

The objectives of the present work were to demonstrate AMSE for phenol, to determine the effect of a transmembrane bulk flow on the diffusional transfer of phenol across the membrane, and to investigate the phenomenon of back-contamination of the wastewater. To produce a uniform

bulk flow across the membrane, we operated a hollow fiber contactor in cocurrent mode with flowrates adjusted to maintain the same transmembrane pressure difference at each end of the contactor. The transmembrane flow could be fixed in direction and magnitude. The wastewater was a phenol solution, and the solvent was an aqueous solution of sodium dodecylsulfate (SDS). This surfactant was chosen because it has a large CMC, thus making the effect of back-contamination more pronounced.

MATERIALS AND METHODS

The experiments were carried out in the apparatus sketched in Fig. 1. The hollow fiber contactor was run in cocurrent mode using two identical flow loops. Liquid was pumped from a stirred reservoir by a peristaltic pump (Masterflex VWR Canlab, Montreal, QC, Canada). Needle valves (VWR Canlab, Montreal, QC, Canada) were used to regulate the pressure in each loop. Parts were connected with PTFE or vinyl tubing of 0.635 cm ID. The differential pressure transducers (OMEGA, Model PX26-015DV, Stamford, CT) had an overall range of ± 103 kPa and an error of ± 1 kPa.

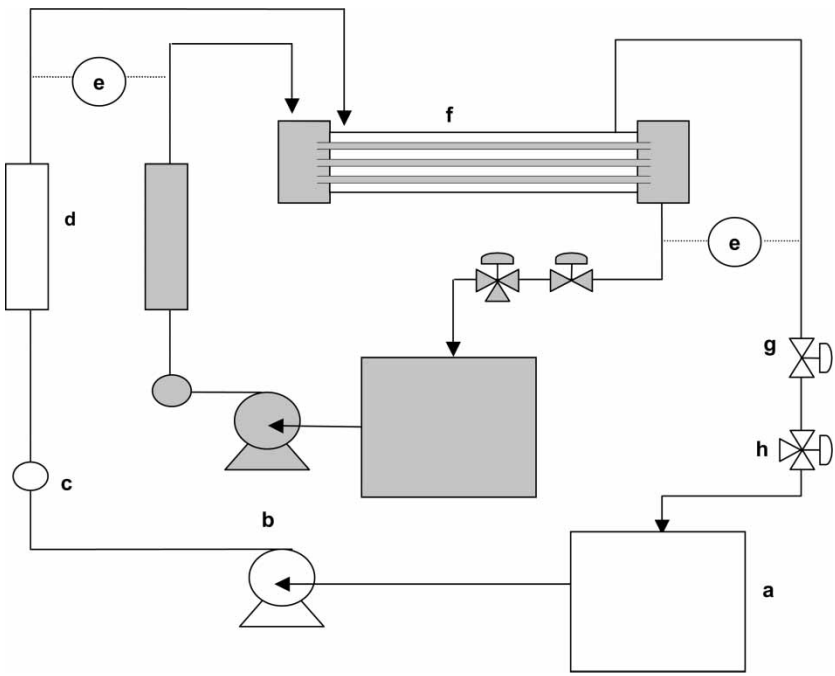

Figure 1. Flowsheet of AMSE setup: a) reservoir, b) peristaltic pump, c) pulse dampener, d) flowmeter, e) differential pressure transducer, f) hollow fiber membrane module, g) needle valve, h) sampling valve.

They were calibrated using a dead-weight tester. The membrane contactors were Xampler™ model polysulfone hollow fiber modules (Amersham Biosciences, Piscataway, NJ). The modules had molecular weight cutoffs (MWCO) of 5, 10, and 30 kDa. Each module contained 30 fibers of 0.5 mm ID, 0.9 mm OD, 30 cm in length, inside a shell of 8 mm ID. The membrane area inside the fibers was 140 cm^2.

Phenol (95–99% pure) and sodium dodecylsulfate (99.9+% pure) were obtained from Fisher Scientific (Montreal QC, Canada), and used as received. The phenol concentration was measured by UV absorption (Varian, CARY-UV, Baltimore, MD) at 260 nm. The surfactant concentration was normally computed from an analysis of total organic carbon (TOC, Rosemount-Dohrman, Model DC-80, Mason, OH), but it was occasionally measured directly by surfactant titration.

Properties of solutions were measured at $22 \pm 2^{\circ}C$. The CMC of SDS solutions was determined by measuring the surface tension of SDS solutions of different concentrations with a ring tensiometer. The CMC was changed by adding salt to SDS solutions at concentrations up to 17.4 g/L NaCl. The kinematic viscosity of SDS solutions was measured with a capillary viscometer. The partition coefficient of phenol between SDS micelles and free phenol was determined by equilibrating a surfactant solution of known concentration with an excess phenol phase.

In extraction experiments, different flowrates were used on each side of the membrane so that the pressure drop was the same along the shell and fiber sides. The mean values of the flowrates were 480 mL/min on the shell side and 120 mL/min on the fiber side with some variation from run to run. The needle valves were used to pressurize one side, thus generating a bulk flow across the membrane. The differential pressures at each end of the module were maintained equal by occasional adjustment of the needle valves. Before starting a run, the solutions in the reservoirs were sampled. During a run the sampling time, the pressure transducer readings, and the flowrate on each side were recorded as each sample was taken. At the end of a run the flow loops were emptied into their respective reservoirs. From the final liquid volume in each reservoir and the total volume of samples, the total volume of liquid on each side of the membrane was calculated.

After each run the module was cleaned in an ultrafiltration mode, first by passing distilled water through the fibers under a pressure of 50–70 kPa, and then through the shell at the same pressure. The pure water flux was checked after every five to seven runs. If the expected flux was not achieved, the module was filled with isopropyl alcohol and left for 24 hours. The water cleaning procedure was then repeated.

Since there was no significant difference between the results when the solvent flowed in the fibers or in the shell, for most experiments the solvent flowed inside the fibers. Three types of experiments were conducted, all at $22 \pm 2^{\circ}C$. The largest number of experiments involved aqueous micellar

extraction of phenol from a wastewater having an initial volume of 2 L and containing approximately 2 g/L of phenol in membrane contactors of 5 K and 10 K MWCO. The solvent was an aqueous SDS solution with an initial volume of 500 mL. A few runs were made without SDS in the solvent to determine the resistance of the membrane to diffusion of phenol. Some experiments were made without phenol in the wastewater to highlight the back-contamination phenomenon. Runs were made with 5 K and 10 K membranes as well as with a 30 K MWCO membrane. The solvent was either SDS in distilled water or SDS in a salt solution. In the latter case, the phenol-free wastewater contained salt at the same concentration as the solvent. In these runs the initial volumes of the wastewater and solvent were 1.5 L. See Cordova-Figueroa (11) for additional details.

At the end of an experiment, two values of the time-averaged bulk flowrate across the membrane were calculated; one from the volumes on the fiber side, the other from the volumes on the shell side. Since these values differed by less than 15%, their average value is used subsequently. The time-averaged bulk flowrate across the membrane, Q, was taken as positive when the flow was from the solvent into the wastewater.

PROPERTIES OF SOLUTIONS

The CMC of SDS in water was measured as 2450 mg/L (8.5 mM), in good agreement with literature data (12). The CMCs of NaCl solutions agreed with Phillips' (13) data. For NaCl concentrations less than 18 g/L, the results are represented with an average deviation of 11% by

$$\frac{C_{surf,CMC}}{C^0_{surf,CMC}} = \exp\left[-1.15\left(\frac{C_{NaCl}}{C^0_{surf,CMC}}\right)^{0.4}\right] \tag{1}$$

where $C^0_{surf,CMC}$ is the CMC of SDS in water, and C_{NaCl} is the concentration of NaCl.

The kinematic viscosity of SDS solutions increased with concentration, but was only 20% larger than that of water at 20 g/L SDS, in agreement with the data of Yang and Matthews (14).

The distribution coefficient of phenol between water and SDS solutions was defined as

$$S = \frac{C_S}{C_W} \tag{2}$$

where C_S is the total concentration of phenol measured in the surfactant solution. Since an excess phenol phase was present, C_W was taken as the solubility of phenol in water. The partition coefficient varied linearly with the surfactant concentration (C_{surf}) in excess of the critical micelle concentration

($C_{surf,CMC}$). For concentrations in g/L, the distribution coefficient is represented with $R^2 = 0.99$ by

$$S = 1.02 + 0.0889\ (C_{surf} - C_{surf,CMC}) \tag{3}$$

AQUEOUS MICELLAR SOLVENT EXTRACTION OF PHENOL

Figure 2 shows the variation of the phenol concentration in the wastewater and in the solvent during extraction across a 5 K MWCO membrane with no time-averaged bulk flow across the membrane ($Q = 0$). Initially, the solvent, which contained 20 g/L SDS, was free of phenol while the wastewater contained approximately 2000 mg/L of phenol. In 3 hours the concentration of phenol in the wastewater was reduced by 300 mg/L, while the concentration of phenol in the solvent increased more rapidly because the volume of solvent was less than the volume of the wastewater. Similar results were obtained with the 10 K MWCO membrane (see Fig. 3).

The extraction of phenol against its overall concentration difference is demonstrated in Fig. 4 for AMSE in a 5 K MWCO contactor. The solvent was a 20 g/L SDS solution initially containing 2100 mg/L of phenol while the wastewater initially contained 2020 mg/L of phenol. The average bulk flowrate across the membrane was zero. The phenol concentration

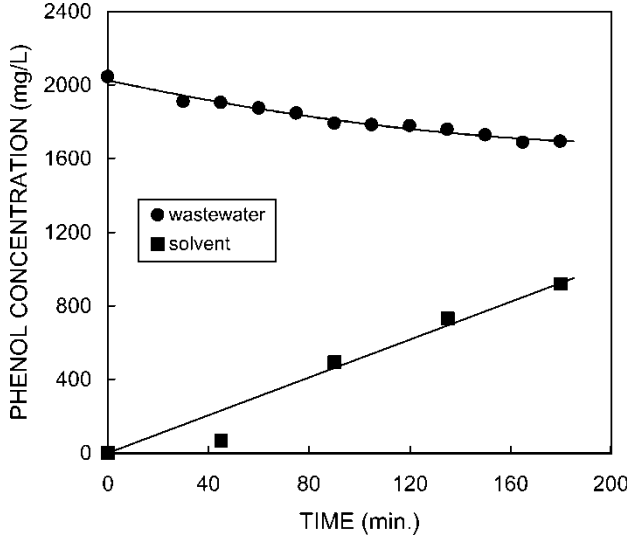

Figure 2. Phenol concentrations versus time for AMSE of phenol with solvent initially phenol-free. (membrane MWCO: 5K; $Q = 0$; initial wastewater concentration: 2160 mg/L phenol; solvent: 20 g/L SDS solution).

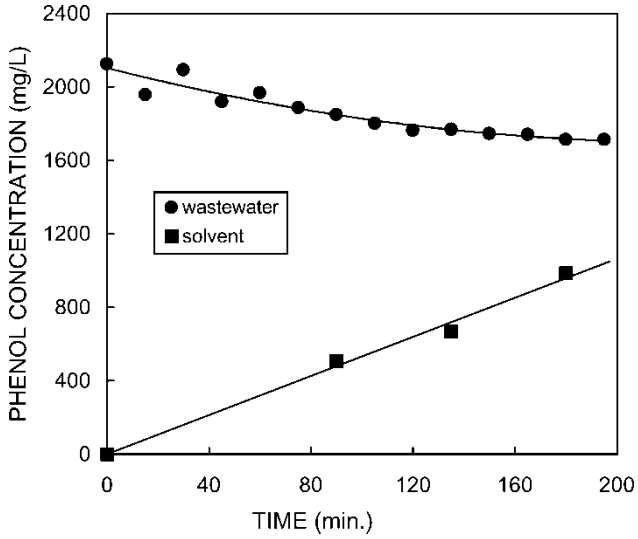

Figure 3. Phenol concentrations versus time for AMSE of phenol with solvent initially phenol-free. (membrane MWCO: 10K; $Q = 0$; initial wastewater concentration: 2030 mg/L phenol; solvent: 20 g/L SDS solution).

decreased in the wastewater and increased in the solvent as it was extracted into the solvent against its overall concentration difference. Without bulk flow, the driving force for phenol transfer across the membrane is the difference between the concentration of phenol in the wastewater and the concentration of free phenol (i.e., phenol not solubilized in the micelles) in the solvent. At the start of the run, when the total concentration of phenol in the solvent was 2100 mg/L, the partition coefficient indicates that the concentration of free phenol was about 800 mg/L. Initially, a free phenol concentration difference of about 1200 mg/L drives the extraction of phenol across the membrane into the solvent. As time passes, the driving force decreases. At 150 min, if the free phenol is in equilibrium with the phenol solubilized in the micelles, the driving force is about 900 mg/L.

Overall Mass Transfer Coefficient

The overall mass transfer coefficient, $K^{\bullet}$, was calculated from the rate of change of the total mass of phenol in one flow loop (e.g., the solvent side) by accounting for the contribution due to the bulk flow. The superscript dot indicates that $K^{\bullet}$ is affected by the bulk flow. The driving force for the transfer of phenol across the membrane was taken as the difference between

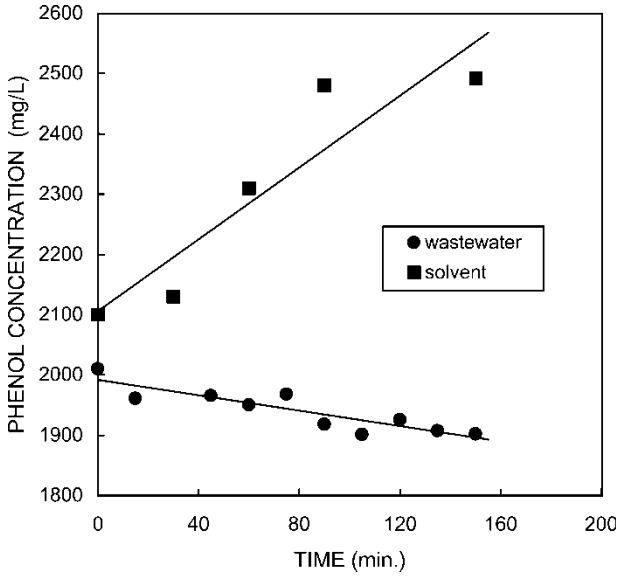

Figure 4. Phenol concentrations versus time for AMSE of phenol with solvent initially loaded with phenol. (membrane MWCO: 5 K; $Q = 0$; initial wastewater concentration: 2010 mg/L phenol; solvent: 20 g/L SDS solution initially containing 2100 mg/L phenol).

the bulk concentration of phenol in the wastewater, C^*, and the bulk concentration of free phenol in the solvent, C_F^{**}. Assuming that the phenol is solubilized into the micelles instantaneously, the free phenol and the solubilized phenol are in equilibrium and the bulk concentration of free phenol in the solvent in the contactor is

$$C_F^{**} = \frac{\bar{C}_S^*}{S} \tag{4}$$

where $\bar{C}_S^*$ is the average total bulk concentration of phenol in the solvent in the contactor and the distribution coefficient, S, is from Eq. (3). On the wastewater side, the change in phenol concentration per pass through the module was less than 1%, so the bulk concentration of phenol in the wastewater was taken as the concentration in the reservoir. On the solvent side, the change in total phenol concentration per pass was about 5–10%, so this change was accounted for in calculating $\bar{C}_S^*$ (11).

Using the solvent side concentration data, $K^\bullet$ was calculated from the following equations. For bulk flow into the wastewater ($Q > 0$):

$$K^\bullet = \frac{\left[dM/dt + QC_F^{**}\right]}{A_1(C^* - C_F^{**})} \tag{5}$$

where M is the total mass of phenol in the solvent flow loop, and A_1 is the inside area of the fibers. For bulk flow into the solvent ($Q < 0$):

$$K^{\bullet} = \frac{[dM/dt + QC^*]}{A_1(C^* - C_F^{**})} \tag{6}$$

The value of M was calculated from the concentration vs. time data and the volume of solution on the solvent side. The time derivative was obtained analytically from a second order polynomial fitted to the M vs. time data. The values of $K^{\bullet}$, which were computed at 15 min intervals scattered around their mean by 5–25%, hence the mean is reported. Similar equations can be derived for the wastewater side of the membrane, thus two values of $K^{\bullet}$ can be calculated.

Figure 5 shows the overall mass transfer coefficient as a function of the flowrate into the wastewater. The points represent the average values of $K^{\bullet}$. Where whiskers are visible, they indicate the values of $K^{\bullet}$ from the solvent and wastewater sides in experiments where these values are not covered by the symbol. The overall mass transfer coefficients for the 5 K MWCO (■) and the 10 K MWCO (●) membranes are similar. The results of experiments with the solvent flowing in the shell side (bars) are similar to those with the solvent in the fibers. Experiments without SDS in the solvent (○, □)

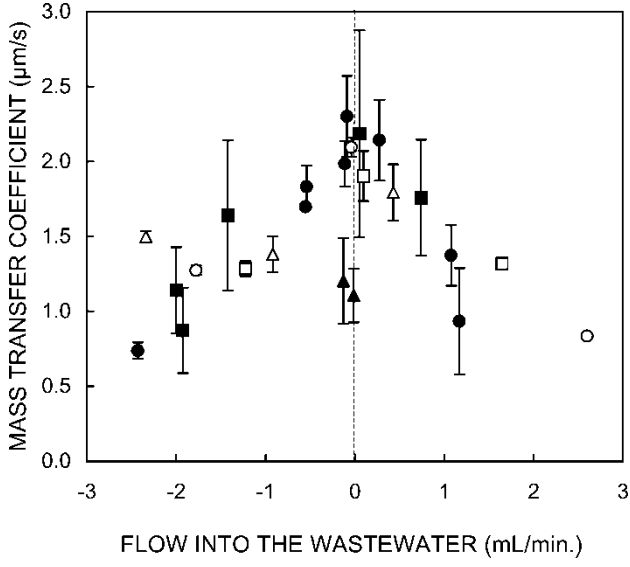

Figure 5. Overall mass transfer coefficient across the membrane as a function of the flowrate across the membrane into the wastewater. (MWCO 5 K: ■ normal CMC, ● CMC lowered by salt, □ distilled water as solvent, ▲ adverse concentration difference; MWCO 10 K: △ normal CMC, ○ distilled water as solvent).

yielded similar results to the ones that used an SDS solvent. The presence of NaCl in the solvent and wastewater had no effect on the overall mass transfer coefficient. The results of experiments with no SDS and experiments with the solvent pumped through the shell indicate that the major resistance to transfer of phenol is the membrane.

The two experiments in which there was an adverse overall concentration difference (one is shown in Fig. 4) gave smaller mass transfer coefficients than those in which the total concentration of phenol in the solvent was always less than the concentration of phenol in the wastewater. With high phenol concentrations in the solvent, it is likely that the phenol crossing the membrane is not solubilized instantaneously. If the solubilization rate is finite, the concentration of free phenol in the solvent is larger than the value from Eq. (4), the driving force is overestimated, and thus $K^{\bullet}$ is underestimated.

The overall mass transfer coefficient was at its highest value, about $2\,\mu m/s$, when there was no bulk flow across the membrane ($Q = 0$). This value compares favorably with overall mass transfer coefficients measured in membrane solvent extraction, a process in which there is no bulk flow. Urtiaga et al. (7) measured overall mass transfer coefficients for extracting phenol from water into solvents consisting of mixtures of kerosene and methyl isobutyl ketone. For mixtures having distribution coefficients around unity, their overall mass transfer coefficients were between 0.6 and $3\,\mu m/s$ for hollow fibers with a wall thickness identical to ours. For extraction across hydrophobic membranes with solvents having large distribution coefficients, where the membrane resistance should be of less importance, overall mass transfer coefficients between 0.2 and $7\,\mu m/s$ have been reported (5, 15).

Bulk flow in either direction reduced the overall mass transfer coefficient essentially symmetrically. A flowrate of $\pm 2\,mL/min$ reduced the mass transfer coefficient to about one-half of its value with no bulk flow. If the value of the bulk flow, measured as the flowrate per unit area, is larger than the zero bulk flow mass transfer coefficient, major changes in the mass transfer coefficient are expected (16). For $Q = \pm 2\,mL/min$, the velocity at the inner surface of the fibers is $\pm 2.4\,\mu m/s$, a value approximately 20% larger than the no bulk flow overall mass transfer coefficient.

ANALYSIS OF THE EFFECT OF BULK FLOW

The concentration profile across the three resistances to mass transfer is sketched in Fig. 6. The analysis is carried out using the stagnant film model (16) for three resistances in series, each resistance of annular cross-section. The dashed lines (at r_0 and r_3) represent the limits of the fictitious fluid films across which the concentration change occurs. The resistances are: (1) the fluid inside the fibers between r_0 and r_1; (2) the membrane between r_1

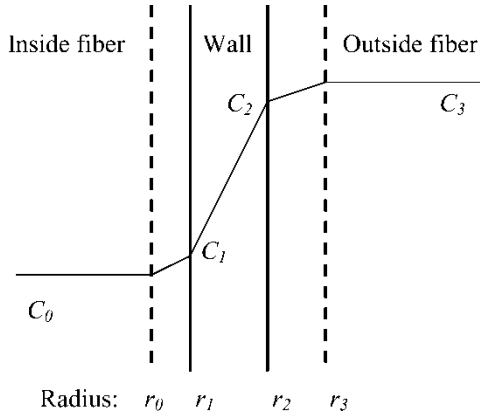

Figure 6. Sketch of concentration profile during AMSE. Dashed lines indicate limits of the fluid films. The superficial velocity (v_i) varies with radius.

and r_2; (3) the fluid outside the fibers (in the shell) between r_2 and r_3. Assuming steady state and constant physical properties, the continuity equation for the solute between r_i and r_j is

$$\left(\frac{v_1 r_1}{r}\right)\frac{dC}{dr} = \frac{D_{i,j}}{r}\left(\frac{1}{r}\frac{d}{dr}\left(r\frac{dC}{dr}\right)\right) \tag{7}$$

where C is the concentration, $D_{i,j}$ is the diffusion coefficient in the phase between r_i and r_j, and v_1 is the velocity at the inside surface of the fibers where $r = r_1$. Solving Eq. (7) with $C = C_i$ at r_i, and $C = C_j$ at r_j, yields the concentration profile:

$$\frac{C - C_i}{C_j - C_i} = \frac{\exp[(v_1 r_1/D_{i,j})\ln(r/r_i)] - 1}{\exp(\beta_{i,j}) - 1} \tag{8}$$

with

$$\beta_{i,j} = \frac{v_1 r_1}{D_{i,j}}\ln\left(\frac{r_j}{r_i}\right) \tag{9}$$

The intermediate concentrations C_1 and C_2 are obtained from the continuity of the fluxes at r_1 and r_2.

For bulk flow out of the fibers ($v_1 > 0$), the overall mass transfer coefficient $K^\bullet$ based on the inside area of the fibers is calculated from the total solute flow at r_0 through the following definition.

$$N_0 A_0 = v_0 A_0 C_0 - D_{0,1}\left(\frac{dC}{dr}\right)_{r=r_0} \equiv v_1 A_1 C_0 + K^\bullet A_1 (C_0 - C_3) \tag{10}$$

where N_0 and A_0 are the flux and area at r_0, respectively, and A_1 is the area at r_1, the inside area of the fibers. Since

$$v_i A_i = Q \tag{11}$$

for any i, the overall mass transfer coefficient is

$$K^{\bullet} = \frac{r_0/r_1}{C_0 - C_3}\left[-D_{0,1}\left(\frac{dC}{dr}\right)_{r_0}\right] \tag{12}$$

For bulk flow into the fibers ($v_1 < 0$), the overall mass transfer coefficient is obtained from the total solute flow at r_3:

$$N_3 A_3 = v_3 A_3 C_3 - D_{2,3} A_3 \left(\frac{dC}{dr}\right)_{r_3} \equiv v_1 A_1 C_3 + K^{\bullet} A_1 (C_0 - C_3) \tag{13}$$

hence

$$K^{\bullet} = \frac{r_3/r_1}{C_0 - C_3}\left[-D_{2,3}\left(\frac{dC}{dr}\right)_{r_3}\right] \tag{14}$$

The overall mass transfer coefficient, calculated through Eq. (12) for $v_1 > 0$ and Eq. (14) for $v_1 < 0$, is symmetrical about $v_1 = 0$. It is represented by

$$\frac{K^{\bullet}}{|v_1|} = \frac{1}{\exp(|\beta_{0,1} + \beta_{1,2} + \beta_{2,3}|) - 1} \tag{15}$$

The quantity $\beta_{i,j}$ can be written in terms of the thickness of the layer, $\delta_{i,j}$:

$$\beta_{i,j} = v_1\left(\frac{r_1 \delta_{i,j}}{D_{i,j}\tilde{r}_{i,j}}\right) \tag{16}$$

where $\delta_{i,j} = r_j - r_i$, and $\tilde{r}_{i,j}$ is the logarithmic mean of r_i and r_j. For the membrane (layer 1,2), $D_{1,2}$ is the effective diffusivity.

Assuming that the thickness of each fluid film is much smaller than its radius, the term in parentheses in Eq. (16) is related to the mass transfer coefficient without bulk flow, $k_{0,1}$ inside the fibers and $k_{2,3}$ outside the fibers:

$$\beta_{0,1} = \frac{v_1}{k_{0,1}} \qquad \text{and} \qquad \beta_{2,3} = \frac{v_1 r_1}{k_{2,3} r_2} \tag{17}$$

For $v_1 \to 0$, $K^{\bullet} \to K$, the overall mass transfer coefficient without bulk flow, and

$$\frac{K^{\bullet}}{K} = \frac{|\beta_{0,1} + \beta_{1,2} + \beta_{2,3}|}{\exp(|\beta_{0,1} + \beta_{1,2} + \beta_{2,3}|) - 1} \tag{18}$$

with

$$\frac{1}{K} = \frac{1}{k_{0,1}} + \frac{\delta_{1,2} r_1}{D_{1,2} \tilde{r}_{1,2}} + \frac{r_1}{r_2 k_{2,3}} \tag{19}$$

Estimation of the Mass Transfer Resistances

The mass transfer coefficient inside the fibers was estimated from the Lêvêque expression for laminar flow in a circular tube (17, 18). With subscript F denoting the fiber side (layer 0,1):

$$Sh_F = 1.62\left[\mathrm{Re}_F Sc_F \left(\frac{d_F}{L}\right)\right]^{1/3} \tag{20}$$

where Sh_F, Re_F and Sc_F are the Sherwood, Reynolds, and Schmidt numbers inside the fibers, respectively, d_F is the inside diameter of the fibers, and L is their length. The Schmidt number was evaluated using the diffusivity values of Yang and Matthews (14). The mean Reynolds number was 144, giving a mass transfer coefficient inside the fibers of 14 μm/s.

The many published empirical correlations for shell side mass transfer coefficients differ widely. Estimates of shell side coefficients should be made from correlations based on experiments with values of important dimensionless variables close to those in our experiments. These variables are: the packing fraction, the fraction of the shell volume occupied by the fibers, $p = 0.38$; the Reynolds number in the shell, $Re_S = 290$; the ratio of the fiber length to the hydraulic diameter of the shell, $L/d_h = 260$; and the ratio of the fiber length to the inside diameter of the shell, $L/d_{shell} = 38$. Three experimental studies match these values reasonably closely. Prasad and Sirkar (19) correlated their data by

$$Sh_S = 5.85(1-p)\left(\frac{d_h}{L}\right) Re_S^{0.53} Sc_S^{0.33} \tag{21}$$

Costello et al. (20) correlated their data by

$$Sh_S = (0.53 - 0.58p)\mathrm{Re}_S^{0.53} Sc_S^{0.33} \tag{22}$$

where the subscript S denotes the shell side (layer 2,3), and Sh_S, and Sc_S are the Sherwood and Schmidt numbers in the shell, respectively. Reviews, like that of Lipnizki and Field (21), show that the Costello et al. mass transfer coefficients are among the highest measured values while the Prasad and Sirkar coefficients are among the lowest. As a general correlation, Lipnizki and Field recommended

$$Sh_S = 1.62(1 + 0.14p^{-1/4})\left[Re_S Sc_S \left(\frac{d_h}{L}\right)\right]^{1/3} \tag{23}$$

Equations (21), (22), and (23) give values of the shell side mass transfer coefficient, k_S, of 4 μm/s, 45 μm/s, and 16 μm/s, respectively.

The fraction of the overall mass transfer resistance represented by the membrane was estimated from Eq. (19) using $k_F = 14\,\mu m/s$ and the three values of k_S. Without bulk flow the experimental overall mass transfer coefficient was approximately 2 μm/s. For the smallest k_S the membrane represented 58% of the overall resistance; for the largest k_S, 83%; for the intermediate k_S, 78%. For our modules, which had fiber walls of 0.2 mm thickness, the rate of mass transfer was largely controlled by diffusion across the membrane. Using fibers with thinner walls would increase the mass transfer rate.

Of the three estimates, we believe that the best is $k_S = 16\,\mu m/s$ because it is consistent with the small effect of shell side flowrate on the overall mass transfer resistance found in previous work on similar modules (10). This value is used in the following analysis. The effective diffusivity of the membrane, D_e, is (22):

$$D_e = D\left(\frac{\varepsilon}{\tau}\right) \tag{24}$$

where D is the diffusion coefficient of phenol, ε is the void fraction of the membrane, and τ is its tortuosity. From the overall mass transfer coefficients measured with distilled water as the solvent, the fiber and shell side mass transfer coefficients, and noting that $D_{1,2} = D_e$, ε/τ was estimated to be 0.4 for both the 5 K and 10 K MWCO membranes.

The effect of the bulk flow on the overall mass transfer coefficient, $K^{\bullet}$, was computed from Eqs. (15)–(17) using the values of k_F, k_S, and ε/τ given above. The computed values are shown as curves in Fig. 7. In runs with micellar solvents, the average difference between the experimental and calculated values was 12%; for runs with water, it was 6%.

BACK-CONTAMINATION

Figure 8 shows the time variation of the SDS concentration in the wastewater for a 10 K MWCO membrane with flowrates, Q, across the membrane ranging from $-1.4\,mL/min$ (from the wastewater into the solvent) to $+4.7\,mL/min$ (from the solvent into the wastewater). The solvent initially contained 20 g/L SDS and the wastewater contained no phenol. The SDS concentration increased with time as surfactant molecules and, perhaps small aggregates, crossed the membrane. For $Q > 0$, bulk flow contributed to the increased back-contamination of the wastewater. For $Q = 0$, SDS crossed the membrane into the wastewater only by diffusion. For $Q < 0$, bulk flow opposed the diffusion, and the back-contamination was reduced.

The concentration of SDS in the wastewater at 180 min is shown in Fig. 9 as a function of the flowrate into the wastewater. In all runs the wastewater was

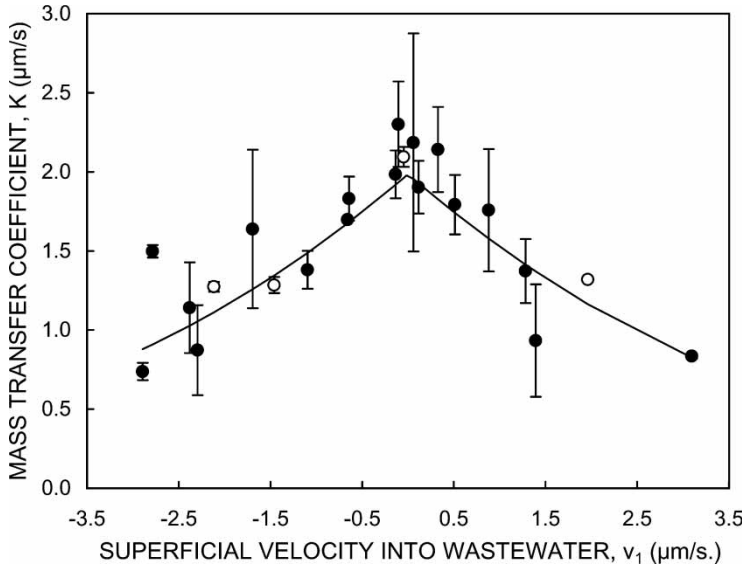

Figure 7. Mass transfer coefficient across the membrane as a function of the superficial velocity across the membrane. The velocity is positive for flow from the solvent into the wastewater. (Solvent: ● SDS solution; ○ distilled water) Curves computed from Equation (15).

free of phenol and the solvent contained 20 g/L of SDS. Since the initial volumes of wastewater and solvent were equal, the maximum concentration of SDS in the wastewater would be one-half of the CMC of the solvent if only surfactant monomers crossed the membrane. With initial volumes of 1.5 L, the maximum concentration would be reached in 180 min for $Q = 8.33$ mL/min.

The open symbols in Fig. 9 show the effect of the MWCO of the membrane for a solvent consisting of SDS in water with a CMC of about 2400 g/L. For all MWCOs, increasing the bulk flow across the membrane increased the concentration of surfactant in the wastewater. Near $Q = 0$, relative to the 5 K membrane, the concentration of SDS was 25% larger for the 10 K membrane and 75% larger for the 30 K membrane. A MWCO of 5 K is about 17 times the molecular weight of a surfactant monomer. Estimating the equivalent molecular weight of a micelle by the product of the micellar aggregation number, about 60 (23), and the molecular weight of SDS, gives approximately 17 K. This estimate suggests that micelles cross the 30 K membrane, and possibly, submicellar aggregates cross the lower MWCO membranes.

Even with the 5 K membrane, there is appreciable back-contamination when $Q \leq 0$ due to diffusion of SDS monomers across the membrane driven by the large CMC of SDS in water. The reduction of back-contamination by lowering the CMC of the surfactant is shown in Fig. 9 by the three filled

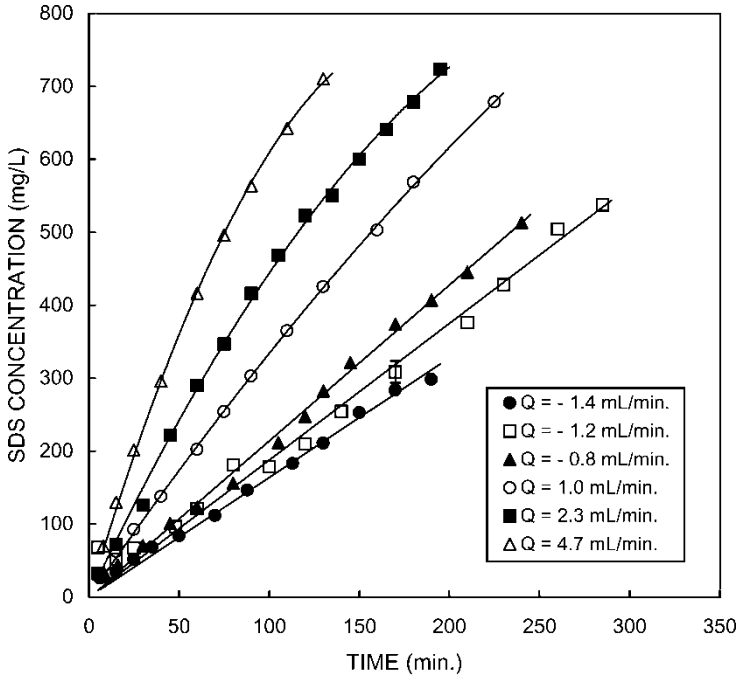

Figure 8. Concentration of SDS in the wastewater versus time for different flowrates across the membrane. (membrane MWCO: 10 K; wastewater: phenol-free; solvent: 20 g/L SDS solution).

symbols for the 10 K MWCO membrane operated with a solvent consisting of 20 g/L SDS dissolved in a salt solution to reduce the CMC. The salt solutions had concentrations of salt (resulting CMC) of 1.2 g/L (1000 mg/L), 2.9 g/L (690 mg/L), and 11.6 g/L (280 mg/L). Experiments conducted with solvents containing 5 g/L SDS and 10 g/L SDS gave results essentially identical to these, confirming that the major cause of back-contamination for the 10 K membrane was due to surfactant monomers crossing the membrane.

The solid curves in Fig. 9 show the variation with flowrate of the concentration of SDS in the wastewater at 180 min, assuming that the only mechanism for transport of surfactant into the wastewater is by bulk flow at the CMC of the solvent. The upper curve is for a CMC of 1000 mg/L; the lower curve, for a CMC of 300 mg/L. Clearly, low CMC surfactants are desirable.

CONCLUSIONS

The aqueous micellar solvent extraction (AMSE) of phenol from a water solution into a solvent consisting of an aqueous micellar SDS solution was

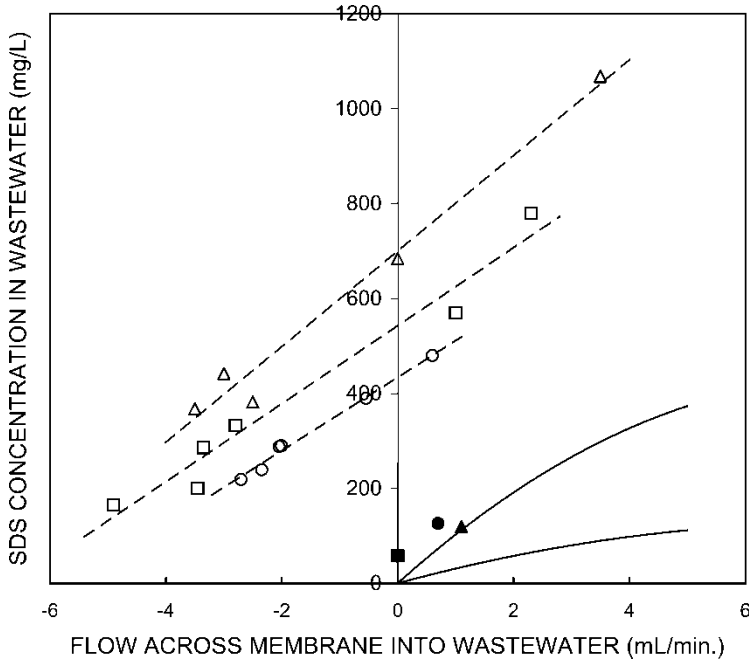

Figure 9. Concentration of SDS in the wastewater after 180 minutes versus flowrate across the membrane for different MWCO membranes and CMC-values for a solvent containing 20 g/L SDS. (open symbols for CMC = 2450 mg/L with MWCO: ○ 5 K, □ 10 K; △ 30 K; filled symbols for MWCO 10 K with CMC: ● 1100 mg/L; ▲ 700 mg/L; ■ 340 mg/L).

carried out in hollow fiber membrane contactors. After accounting for transport across the membrane by bulk flow, the major resistance to diffusive mass transfer of phenol was the membrane. The effect of a bulk flow across the membrane was symmetric about zero bulk flow: flow in either direction reduced the overall mass transfer coefficient. The magnitude of the reduction was described well by the film theory.

Back-contamination of the wastewater with SDS was increased by bulk flow across the membrane into the wastewater and decreased by flow in the reverse direction. Lowering the CMC of the solvent reduced back-contamination dramatically, while the surfactant concentration in the solvent had no effect. A membrane with a MWCO of 5 K gave lower back-contamination without reducing the rate of transfer of phenol across the membrane.

To reduce back-contamination, the contactor should be operated with the smallest transmembrane pressure difference that is manageable. If the flow in the module is cocurrent, the pressures should be matched closely. If the flow in the module is countercurrent, the condition of zero net flow over the module

should be used. The degree of back-contamination of the treated water is best indicated by the mass concentration, e.g., mg/L. A surfactant with a small CMC in mass concentration units is preferred. The choice of the MWCO of the membrane is a compromise between good rejection of surfactant aggregates by the membrane and unhindered diffusion of solute across the membrane. To reject the surfactant aggregates, a small MWCO is desirable, but too small a MWCO may hinder diffusion of the solute. A reasonable MWCO window of operation might be between ten times the molecular weight of the solute and ten times the molecular weight of the surfactant.

NOMENCLATURE

A_i	Area at location i
C	Phenol concentration
C^*	Phenol concentration in the wastewater
C_F^{**}	Free phenol concentration in the solvent
D	Diffusivity of the solute
D_e	Effective diffusivity of the solute in the membrane
d_F	Internal diameter of fiber
d_h	Hydraulic diameter of the shell
d_{shell}	Inside diameter of shell
K	Overall mass transfer coefficient without bulk flow
$K^\bullet$	Overall mass transfer coefficient in the presence of bulk flow
L	Length of fibers
M	Total mass of phenol in solvent or wastewater flow loop
p	Packing fraction of shell
Q	Flowrate across the membrane into the wastewater
r	Radius
r_i	Radius of location i
$\tilde{r}_{i,j}$	Logarithmic mean radius of r_i and r_j, $\tilde{r}_{i,j} = (r_j - r_i)/\ln(r_j/r_i)$
Re	Reynolds number, $Re_F = d_F\, u_F\, \rho/\mu$ or $Re_S = d_h\, u_s\, \rho/\mu$
S	Phenol partition coefficient
Sc	Schmidt number, $Sc = \mu/\rho D$
Sh	Sherwood number, $Sh_F = k_F\, d_i/D$ or $Sh_S = k_S\, d_h/D$
t	Time
u_F	Mean axial velocity inside a fiber
u_S	Mean axial velocity in the free area of the shell
v_i	Velocity in the radial direction at location i

Greek Letters

$\beta_{i,j}$	parameter defined in Eq. (16)
$\delta_{i,j}$	Thickness of layer between locations i and j

ε	Membrane void fraction
μ	Viscosity
ρ	Density
τ	Membrane tortuosity

Subscripts

0	Internal boundary of fiber side film
1	Internal (fiber side) membrane surface
2	External (shell side) membrane surface
3	External boundary of shell side film
F	Fiber side
S	Shell side

ACKNOWLEDGMENT

The Natural Sciences and Engineering Research Council of Canada provided financial support.

REFERENCES

1. Prasad, R. and Sirkar, K.K. (1987) Microporous membrane solvent extraction. *Sep. Sci. Technol.*, 22: 619–640.
2. Prasad, R. and Sirkar, K.K. (1992) Membrane-based solvent extraction. In *Membrane Handbook*; Ho, W. and Sirkar, K.K., eds.; Van Nostrand Reinhold: New York, 727–763.
3. Gabelman, A. and Hwang, S.T. (1999) Hollow fiber membrane contactors. *J. Membrane Sci.*, 159: 61–106.
4. Gawroński, R. and Wrzesińska, B. (2000) Kinetics of solvent extraction in hollow-fiber contactors. *J. Membrane Sci.*, 168: 213–222.
5. González-Muñoz, M.J., Luque, S., Álvarez, J.R., and Coca, J. (2003) Recovery of phenol from aqueous solutions using hollow fiber contactors. *J. Membrane Sci.*, 213: 181–193.
6. Wang, Y., Chen, F., Wang, Y., Luo, G., and Dai, Y. (2003) Effect of random packing on shell-side flow and mass transfer in hollow fiber module described by normal distribution function. *J. Membrane Sci.*, 216: 81–93.
7. Urtiaga, A.M., Ortiz, M.I., Salazar, E., and Irabien, J.A. (1992) Supported liquid membranes for separation-concentration of phenol. 1. Viability and mass transfer evaluation. *Ind. Eng. Chem. Research*, 31: 877–886.
8. Yun, C.H., Prassad, R., and Sirkar, K.K. (1992) Membrane solvent extraction for the removal of priority organic pollutants from aqueous waste streams. *Ind. Eng. Chem. Research*, 31: 1709–1717.
9. Hurter, P.A. and Hatton, T.A. (1992) Solubilization of polycyclic aromatic hydrocarbons by poly(ethylene oxide-propylene oxide) block copolymer micelles: effects of polymer structure. *Langmuir*, 8: 1291–1299.
10. Marx, S. and Weber, M.E. (2002) Extraction of a dissolved organic contaminant from water into an aqueous surfactant solution across a microporous membrane. *Can. J. Chem. Eng.*, 80: 224–230.

11. Cordova-Figueroa, M. (2003) Micellar-enhanced extraction of phenol from wastewater. McGill University: Montreal, QC, Canada, M. Eng. Thesis.
12. Elworthy, P.H. and Mysels, K.J. (1966) The surface tension of sodium dodecylsulfate solutions and the phase separation model of micelle formation. *J. Colloid Sci.*, 21: 331–347.
13. Phillips, J.N. (1955) The energetics of micelle formation. *Trans. Faraday Soc.*, 51: 561–569.
14. Yang, X. and Matthews, M.A. (2000) Diffusion coefficients of three organic solutes in aqueous sodium dodecyl sulfate solutions. *J. Colloid Interface Sci.*, 229: 53–61.
15. Stevanović, S.M., Mitrović, M.V., and Korenman, Y.I. (1999) Membrane extraction of phenol with linear monoacyl cyclohexane. *Sep. Sci. Technol.*, 34: 651–663.
16. Bird, R.B., Stewart, W.E., and Lightfoot, E.N. (2002) *Transport Phenomena*, 2nd Ed.; John Wiley & Sons: New York, 703–716.
17. Wickramasinghe, S.R., Semmens, M.J., and Cussler, E.L. (1992) Mass transfer in various hollow fiber geometries. *J. Membrane Sci.*, 69: 235–250.
18. Reed, B.W., Semmens, M.J., and Cussler, E.L. (1995) Membrane Contactors. In *Membrane Separations Technology: Principles and Applications*; Noble, R.D. and Stern, S.A., eds.; Elsevier: Amsterdam, 467–498.
19. Prasad, R. and Sirkar, K.K. (1988) Dispersion-free solvent extraction with microporous hollow-fiber modules. *AIChE J.*, 34: 177–188.
20. Costello, M.J., Fane, A.G., Hogan, P.A., and Schofield, R.W. (1993) The effect of shell side hydrodynamics on the performance of axial hollow fiber modules. *J. Membrane Sci.*, 80: 1–11.
21. Lipnizki, F. and Field, R.W. (2001) Mass transfer performance for hollow fiber modules with shell-side axial flow: using an engineering approach to develop a framework. *J. Membrane Sci.*, 193: 195–208.
22. Cussler, E.L. (1997) *Diffusion: Mass Transfer in Fluid Systems*, 2nd Ed.; Cambridge University Press: Cambridge, 173.
23. Lianos, P. and Zana, R. (1980) Use of pyrene excimer formation to study the effect of NaCl on the structure of sodium dodecyl sulphate micelles. *J. Phys. Chem.*, 84: 3339–3341.